

University of Groningen

Optical properties of disordered molecular aggregates

Fidder, Henk; Knoester, Jasper; Wiersma, Douwe A.

Published in:
The Journal of Chemical Physics

DOI:
[10.1063/1.461317](https://doi.org/10.1063/1.461317)

IMPORTANT NOTE: You are advised to consult the publisher's version (publisher's PDF) if you wish to cite from it. Please check the document version below.

Document Version
Publisher's PDF, also known as Version of record

Publication date:
1991

[Link to publication in University of Groningen/UMCG research database](#)

Citation for published version (APA):

Fidder, H., Knoester, J., & Wiersma, D. A. (1991). Optical properties of disordered molecular aggregates: a numerical study. *The Journal of Chemical Physics*, 95(11), 7880-7890. <https://doi.org/10.1063/1.461317>

Copyright

Other than for strictly personal use, it is not permitted to download or to forward/distribute the text or part of it without the consent of the author(s) and/or copyright holder(s), unless the work is under an open content license (like Creative Commons).

The publication may also be distributed here under the terms of Article 25fa of the Dutch Copyright Act, indicated by the "Taverne" license. More information can be found on the University of Groningen website: <https://www.rug.nl/library/open-access/self-archiving-pure/taverne-amendment>.

Take-down policy

If you believe that this document breaches copyright please contact us providing details, and we will remove access to the work immediately and investigate your claim.

Downloaded from the University of Groningen/UMCG research database (Pure): <http://www.rug.nl/research/portal>. For technical reasons the number of authors shown on this cover page is limited to 10 maximum.

Optical properties of disordered molecular aggregates: A numerical study

Henk Fidler, Jasper Knoester, and Douwe A. Wiersma

*University of Groningen, Department of Chemistry, Ultrafast Laser and Spectroscopy Laboratory,
Nijenborgh 16, 9747 AG Groningen, The Netherlands*

(Received 7 June 1991; accepted 19 August 1991)

We present results of numerical simulations on optical properties of linear molecular aggregates with diagonal and off-diagonal disorder. In contrast to previous studies, we introduce off-diagonal disorder indirectly through Gaussian randomness in the molecular positions; this results in a strongly asymmetric distribution for the interactions. Moreover, we do not restrict to nearest-neighbor interactions. We simultaneously focus on several optical observables (absorption linewidth and line shift and superradiant behavior) and on the density and the localization behavior of the eigenstates (Frenkel excitons). The dependence of these optical properties on the disorder is investigated and expressed in terms of simple power laws. For off-diagonal disorder, such a study has not been performed before. In the case of diagonal disorder, we show that, in particular, the superradiant decay rate of the aggregates may be strongly affected by the inclusion of non-nearest-neighbor interactions. Recent results of absorption line shape, superradiant emission, and resonance light-scattering measurements on pseudoisocyanine aggregates can be understood on the basis of these calculations.

I. INTRODUCTION

Presently, there is considerable interest in the optical dynamics of low-dimensional systems¹⁻¹⁸ such as quantum wells,³ Langmuir-Blodgett films,⁴⁻⁶ polymers,⁷⁻⁹ and molecular aggregates.^{6,10-18} As intermediates between single molecules and bulk phases, these systems are ideal to investigate the changes of physical properties between these two extremes. Moreover, many fundamental and technical aspects of these systems are unique and interesting in their own right. In this paper, we study optical properties of one-dimensional molecular aggregates. This study is motivated by the extensive experimental work performed in our group on the *J* aggregates of pseudoisocyanine^{6,10-14} (PIC). However, our results are relevant to any other linear molecular aggregate described by Frenkel excitons. To stress this, our theory is cast in a general form, without specific choices for quantities that would only apply to PIC.

In perfectly ordered (homogeneous) aggregates the excited electronic eigenstates extend over the entire chain. This complete delocalization of the molecular excitations is reflected in the fact that the radiative decay rate of the lowest exciton band state scales linearly with the chain length. In practice, however, the aggregates contain some amount of disorder, which may severely affect the delocalization behavior and the observed optical properties. Disorder can either be diagonal, meaning a spread in transition frequencies of the individual molecules, or off-diagonal, expressing a variation in the intermolecular interactions. Diagonal disorder corresponds to the situation of inhomogeneous broadening due to different molecular surroundings. Off-diagonal or interaction disorder, on the other hand, implies physical irregularity of the chain itself. This irregularity can exist in the positions and (or) the orientations of the molecules.

It is an important problem to understand how the optical properties, such as the absorption line shape and the superradiant emission rate, depend on the disorder and the aggregate chain length. On the one hand, this may help to

assess the experimentally often inaccessible and uncontrollable chain length; on the other hand, this may guide technological developments.^{19,20} Furthermore, it is of interest to study interrelationships between the various optical properties of aggregates.

Over the past decades, much work has been devoted to diagonal disorder in chains with nearest-neighbor interactions.^{17,18,21-27} One well-known result is that in one dimension no Anderson localization transition occurs, i.e., any amount of diagonal disorder localizes the electronic wave functions on a finite interval of an infinite chain.^{21,22} This general and rather formal result, however, still leaves many questions concerning the exact localization length, optical properties, and effects of finite chain lengths unanswered.

Klafter and Jortner²³ were the first to show that the asymmetric absorption line shape of one-dimensional excitonic systems can be explained by Gaussian diagonal disorder. Furthermore, Knapp¹⁷ assessed that for small inhomogeneity, the absorption line shape is narrowed by a factor $N^{1/2}$ for aggregates of N molecules as a result of the intermolecular interactions. This "exchange narrowing" results from the fact that the delocalized excitons average over the Gaussian molecular inhomogeneities within each aggregate. Other important scaling laws of optical properties with the chain length and (or) the spread in the diagonal disorder have been derived by, e.g., Schreiber and Toyozawa²⁴ (absorption line) and more recently by Spano and Mukamel¹⁸ (superradiant emission) and Boukahlil and Huber²⁶ (absorption line).

Off-diagonal disorder has been investigated less extensively. It was long thought that diagonal and off-diagonal disorder would lead to completely comparable features. During the seventies, however, studies of the density^{28,29} and the localization behavior^{29,30} of the aggregate eigenstates, invalidated this belief. Weissmann and Cohan²⁸ showed that in the presence of off-diagonal disorder, the density-of-states peaks at the center of the one-dimensional exciton band. Theodorou and Cohen²⁹ substantiated this

claim and derived that the eigenstates at this peak (and only these) remain extended irrespective of the amount of off-diagonal disorder and the shape of the disorder distribution. It is interesting that, in contrast with the one-dimensional situation, Bauer *et al.*³¹ claimed that in three dimensions both diagonal and off-diagonal (topological and quantum percolation) disorder shows the same localization behavior.

The *simultaneous* inclusion of diagonal and off-diagonal disorder has so far received very little attention. Economou and Cohen³² concluded that, in this case, all eigenstates are localized. Recently, however, Dunlap *et al.*³³ showed that if the diagonal and off-diagonal disorder are mutually correlated, delocalized eigenstates may exist irrespective of the amount of disorder.

In this paper we report results from extensive numerical simulations on the one-dimensional Frenkel exciton Hamiltonian with diagonal and off-diagonal disorder. An important difference between our study and previous work is that we investigate several quantities of interest simultaneously: the absorption linewidth and line shift, the superradiant behavior, the density of states, and the degree of localization of the eigenstates. Not only do we establish the behavior of these quantities as a function of the disorder (and the chain length), we also try to relate them to each other, in order to create a better picture of the eigenstates in the disordered aggregates. Moreover, in contrast to all previous work,^{17,18,21-30,32,33} we include *all* dipolar couplings between the molecules within the chains. Effects thereof on the exciton band structure and the delocalization behavior are discussed. The contents of this paper is as follows. In Sec. II we give the general theoretical framework and define the various quantities used in our analysis. Next, Secs. III and IV contain the numerical results for diagonal and off-diagonal disorder, respectively. Finally, in Sec. V we summarize our results.

II. THEORY

We consider a linear chain of N identical polarizable two-level molecules. Neglecting phonons and restricting to states with at most one excitation on the chain, this system is described by the exciton Hamiltonian

$$H = \sum_n (\langle \epsilon \rangle + D_n) |n\rangle \langle n| + \sum_{n,m} \sum_{n \neq m} J_{nm} |m\rangle \langle n| \\ \equiv \sum_n \sum_m H_{nm} |m\rangle \langle n|. \quad (2.1)$$

Here $|n\rangle$ denotes the state in which molecule n ($n = 1, \dots, N$) is excited and all other molecules are in the ground state. $\langle \epsilon \rangle$ stands for the average molecular excitation energy and D_n is the (static) inhomogeneous offset energy of molecule n , reflecting the effect of disorder imposed by the surrounding host medium (diagonal disorder). In practice, the D_n may be considered random variables, taken from an appropriate distribution (Sec. III). Henceforth, all energies will be given relative to $\langle \epsilon \rangle$, so that this term is dropped from the Hamiltonian. J_{nm} in Eq. (2.1) is the instantaneous intermolecular interaction (transfer integral) between molecules n and m , which we will assume to be of dipolar origin. We confine ourselves to the case where all molecules have equal and

parallel transition dipole moments of magnitude μ_{mon} that make an angle β with the chain direction. We then have

$$J_{nm} = \mu_{\text{mon}}^2 (1 - 3 \cos^2 \beta) / r_{nm}^3, \quad (2.2)$$

where $r_{nm} \equiv |\mathbf{r}_n - \mathbf{r}_m|$ is the distance between molecules n and m . The positions \mathbf{r}_n of the individual molecules are fixed (no phonons), but do not necessarily form a regular one-dimensional lattice. Instead, we will allow the \mathbf{r}_n to be distributed around average lattice positions in order to account for configurational disorder. This leads to off-diagonal disorder: disorder in the interactions J_{nm} (Sec. IV). The interaction may be parametrized in a compact way as

$$J_{nm} = -J(a/r_{nm})^3, \quad (2.3)$$

with $-J$ the interaction between two molecules at the average nearest-neighbor distance, which is denoted as a . J serves as the unit of energy in this paper.

As is well known, intermolecular interactions form the driving force for delocalization of the electronic eigenstates over the entire chain. Both diagonal and off-diagonal disorder, on the other hand, tend to localize the eigenstates.^{21,22,29,30,32,34} The effect of both types of disorder on the eigenstates and optical properties of aggregates will be studied separately in this paper.

For a particular realization of the disorder, the eigenstates are found by diagonalizing the $N \times N$ matrix H_{nm} . Then, the j th eigenvalue \mathcal{E}_j gives the energy of the eigenstate j , whereas the normalized j th eigenvector $\mathbf{a}_j = (a_{j1}, \dots, a_{jN})$ specifies its wave function,

$$|\Psi_j\rangle = \sum_{n=1}^N a_{jn} |n\rangle. \quad (2.4)$$

The localized or delocalized nature of the various eigenstates is reflected in the optical and radiative properties of the aggregates (absorption bands, superradiant emission). In order to study these properties, we need to consider the interaction of the aggregate with the transverse radiation field. The coupling of the radiation field mode of wave vector \mathbf{k} to the eigenstate j is governed by

$$\sum_{n=1}^N a_{jn} \mu_{\text{mon}} \exp(-i\mathbf{k} \cdot \mathbf{r}_n).$$

We will, however, restrict our study to aggregates with length L small compared to an optical wavelength ($|\mathbf{k}|L \ll 1$), so that the coupling constant reduces to the transition dipole

$$\mu_j = \sum_{n=1}^N a_{jn} \mu_{\text{mon}}. \quad (2.5)$$

The aggregate is thus considered as one giant multilevel molecule in the dipole approximation. The oscillator strength which determines the one-photon absorption and the radiative lifetime of the j th eigenstate is then proportional to μ_j^2 , and is easily obtained once the eigenvectors have been calculated.

The approach outlined above to evaluate the optical response of aggregates thus exists of first diagonalizing the exciton Hamiltonian (2.1) with instantaneous intermolecular interactions and subsequently determining the coupling of the exciton eigenstates to the radiation field. This method

most closely connects to the vast literature dealing with localization properties of disordered exciton systems and is correct for small systems ($|k|L \ll 1$). In an alternative, more general approach,¹⁸ one includes the coupling with the radiation field from the very start. Formal elimination of the radiation field then leads to a reduced equation of motion for the exciton variables, the well-known superradiance master equation.³⁵ The most important ingredient in this equation is the fully retarded intermolecular dipole-dipole interaction. The real part of this interaction contains corrections to the instantaneous interaction J_{nm} which are proportional to $1/r_{nm}^2$ and $1/r_{nm}$. In the near zone, which applies to aggregates small compared to an optical wavelength, these corrections may be neglected, however. The imaginary part of the retarded interaction describes the (collective) radiative decay; in the near zone this contribution is independent of the intermolecular separation and the radiative decay is equally well described by the transition dipole Eq. (2.5).

Before turning to the general case of disorder, it is useful for future reference to discuss several results for the eigenstates of perfectly ordered systems ($D_n = 0$, $r_n = na$). If only nearest-neighbor interactions are taken into account ($J_{nm} = -J$ if $|n - m| = 1$, $J_{nm} = 0$ otherwise), the Hamiltonian (2.1) can be diagonalized exactly for the ordered linear chain, leading to the eigenfunctions³⁶

$$|\psi_j^L\rangle = \left(\frac{2}{N+1}\right)^{1/2} \sum_{n=1}^N \sin\left(\frac{\pi j n}{N+1}\right) |n\rangle, \quad (2.6a)$$

with energies

$$\mathcal{E}_j^L = -2J \cos\left(\frac{\pi j}{N+1}\right) \quad (2.6b)$$

($j = 1, \dots, N$). From Eq. (2.6a) it may be shown that only eigenstates with j odd have oscillator strength,³⁶

$$(\mu_j^L)^2 = \left(\frac{2\mu_{\text{mon}}^2}{N+1}\right) \cot^2\left(\frac{\pi j}{2(N+1)}\right), \quad j = \text{odd} \\ (\mu_j^L)^2 = 0, \quad j = \text{even}. \quad (2.7)$$

Elementary analysis of these expressions reveals that the state $j = 1$ contains an overwhelming part of the total oscillator strength $N\mu_{\text{mon}}^2$ (up to 81% for $N \gg 1$), leading to superradiant emission and domination of the absorption spectrum by this state. The oscillator strengths of higher states drop off as $1/j^2$ for $j \ll N$. The exciton band Eq. (2.6b) extends from $\mathcal{E} = -2J$ to $\mathcal{E} = +2J$, and is symmetric around $\mathcal{E} = 0$. For $J > 0$, the $j = 1$ state lies at the bottom of the band (direct band edge), whereas, for $J < 0$, this state is located at the top of the band. In the remainder of this paper we will assume that $J > 0$.

Analytical diagonalization of the linear-chain problem with *all* dipolar interactions taken into account (instead of just the nearest-neighbor couplings), presents a difficult problem. Straightforward numerical diagonalization, however, reveals that the wave functions are very similar to the j states of Eq. (2.6a). It turns out that as a result of the additional interactions, the oscillator strength of the lowest band state increases to about 83% of the total (for $N = 250$). Furthermore, the exciton band now shows a marked asymmetry around $\mathcal{E} = 0$: the lower edge is found at $\mathcal{E} = -2.403J$,

and the upper edge at $\mathcal{E} = 1.803J$. The origin of this asymmetry lies in the extra interactions over an even number of lattice spacings ($|m - n| = 2, 4, \dots$). The increase of the total band width from $4J$ to $4.206J$, on the other hand, results from the extra interactions over an odd number of lattice spacings ($|m - n| = 3, 5, \dots$). This may be assessed by studying aggregates with periodic boundary conditions (circular aggregates), for which even in the case of arbitrary interactions the eigenstates are easily obtained using Fourier analysis,

$$|\psi_j^c\rangle = N^{-1/2} \sum_{n=1}^N e^{2\pi i(jn/N)} |n\rangle, \quad (2.8a)$$

with energies

$$\mathcal{E}_j^c = 2 \sum_m^* J_{1m} \cos\left(\frac{2\pi j(m-1)}{N}\right) \quad (2.8b)$$

($j = 0, \dots, N-1$). The asterisk on the summation in Eq. (2.8b) indicates that it runs from $m = 2$ to $m = (N+1)/2$ (N taken odd). The circular aggregate is often taken as a model for linear aggregates, because of the possibility to calculate many of its properties analytically. It is believed that the general features for large ($N \gg 1$) linear and circular aggregates are identical. For instance, also in the circular case the lowest state (now labeled $j = 0$) is superradiant and contains rigorously all oscillator strength: $\mu_j^c = N^{1/2} \mu_{\text{mon}} \delta_{j,0}$. We note that the fact that different oscillator strengths are found for the lowest states of the linear and circular aggregate (81% and 100%, respectively) does not contradict the idea that for $N \rightarrow \infty$ both models should give identical results. The reason is that, for $N \rightarrow \infty$, all other states of the linear chain that carry oscillator strength become degenerate with the state $j = 1$, so that the *spectral density* of the oscillator strength becomes a δ function at the lower band edge, just as in the case of the circular aggregate.

If only nearest-neighbor interactions are taken into account, the density of states (DOS) in the exciton band Eq. (2.8b) is again symmetric around the band center located at $\mathcal{E} = 0$ ($j = N/4$ and $j = 3N/4$). Since most theories restrict to nearest-neighbor interactions, this symmetry is usually taken for granted. In fact, it follows from Eq. (2.8b) that inclusion of any longer-range interactions between molecules separated by an *odd* number of sites increases the width of the band, but maintains this symmetry, because $\cos[2\pi j(m-1)/N]$ is odd with respect to $j = N/4$ and $j = 3N/4$ if $m-1$ is odd. Interactions over an *even* number of sites, however, introduce an asymmetry in the DOS, because $\cos[2\pi j(m-1)/N]$ is even with respect to $j = N/4$ and $j = 3N/4$ for $m-1$ even. It is easily derived from Eq. (2.8b) that the bottom of the band ($j = 0$) is located at

$$2 \sum_m^* J_{1m}$$

and the top ($j = N/2$) at

$$2 \sum_m^* (-1)^{m-1} J_{1m}.$$

For a circular aggregate of 251 molecules and with interactions of the form Eq. (2.3), this leads to predictions of $\mathcal{E} = -2.404J$ and $\mathcal{E} = 1.803J$ for the lower and the upper

band edge, respectively. These figures are in excellent agreement with the above mentioned numerical diagonalization of the linear chain.

In the general case of disorder, it is, of course, impossible to diagonalize the Hamiltonian analytically. Every realization of the disorder yields a different set of energies \mathcal{E}_j and eigenvectors \mathbf{a}_j . Observables, such as the absorption spectrum and the enhancement of the radiative decay rate relative to the single molecule (superradiance), are averages over many different realizations of the disorder. We calculated these properties by a straightforward numerical simulation, in which disordered aggregates of N molecules were randomly generated according to prescribed distributions of the inhomogeneity (Sec. III) or the molecular positions (Sec. IV). Subsequently, for every aggregate the Hamiltonian (2.1) was diagonalized numerically. All numerical routines were taken from Ref. 37. The stability of the diagonalization program was tested against the conservation of the trace of the Hamiltonian and the total oscillator strength of the eigenstates; errors appeared to be smaller than 0.01% in all cases. The diagonalization yields real eigenvalues and eigenvectors (H_{nm} is a real and symmetric matrix).

In the remainder of this section, we will introduce the observables on which we focused in our simulations. The absorption line-shape function is calculated as

$$\mathcal{A}(\mathcal{E}) = \frac{1}{N} \left\langle \sum_j \Delta(\mathcal{E} - \mathcal{E}_j) \mu_j^2 \right\rangle, \quad (2.9)$$

where the angular brackets indicate an average over an ensemble of randomly generated aggregates and the sum over j runs over all eigenstates of the individual aggregates within this ensemble. The function Δ is defined as

$$\begin{aligned} \Delta(\mathcal{E} - \mathcal{E}_j) &= 1/R \quad \text{for } |\mathcal{E} - \mathcal{E}_j| < R/2, \\ \Delta(\mathcal{E} - \mathcal{E}_j) &= 0 \quad \text{otherwise.} \end{aligned} \quad (2.10)$$

Here R is the resolution of the spectrum, which has to be taken large enough to smooth out statistical fluctuations and small enough to maintain the salient features of the spectrum. In an exact calculation, Δ should be replaced by a Dirac δ function. Analogously to the absorption spectrum, the normalized aggregate density of states is calculated as

$$\rho(\mathcal{E}) = \frac{1}{N} \left\langle \sum_j \Delta(\mathcal{E} - \mathcal{E}_j) \right\rangle. \quad (2.11)$$

Next, we define two measures for the enhancement of the radiative decay rate relative to the monomer spontaneous emission rate. The first measure is the average oscillator strength per state at energy \mathcal{E} , defined as²⁴

$$\mu_{\text{av}}^2(\mathcal{E}) = \mathcal{A}(\mathcal{E})/\rho(\mathcal{E}). \quad (2.12)$$

It appears from our simulations that with decreasing energy \mathcal{E} , this quantity has a steep increase near the absorption maximum, then remains roughly constant over an energy interval which extends to below the absorption peak, and then slowly decreases towards lower energies (cf. Ref. 24). We therefore take $\max(\mu_{\text{av}}^2(\mathcal{E})/\mu_{\text{mon}}^2)$ as a measure for the enhancement of the radiative rate as observed in low-temperature fluorescence experiments, provided that the excitation population has thermalized. We note that the relevance of this measure critically depends on the dynamics of the

specific system under consideration. If the radiative rate is obtained from photon echo experiments, a different enhancement is found. Disorder introduces a distribution of oscillator strength per state at every energy and the nonlinear (four-wave mixing) nature of photon echo experiments increases the relative contribution of eigenstates with higher oscillator strength. We define an effective echo decay rate μ_{echo}^2 as the $1/e$ "time" of the echo field amplitude

$$E_{\text{echo}}(\mathcal{E}) \propto \left\langle \sum_j \Delta(\mathcal{E} - \mathcal{E}_j) \mu_j^4 \exp(-\mu_j^2 t) \right\rangle. \quad (2.13)$$

Here, \mathcal{E} is the laser frequency. Of course, Eq. (2.13) only includes the radiative part of the echo decay; phonon contributions have been neglected.

Finally, it is useful to have independent quantitative information on the localization properties of the aggregate eigenstates. Following Thouless³⁸ and Schreiber and Toyozawa,²⁴ we therefore define the degree of localization (inverse participation ratio) for the states at energy \mathcal{E} as

$$\mathcal{L}(\mathcal{E}) = \frac{1}{N} \left\langle \sum_j \Delta(\mathcal{E} - \mathcal{E}_j) \left(\sum_{n=1}^N a_{jn}^4 \right) \right\rangle / \rho(\mathcal{E}). \quad (2.14)$$

A state localized on a single molecule has $\mathcal{L}(\mathcal{E}) = 1$, whereas for the completely delocalized states Eq. (2.6a) of the linear chain, $\mathcal{L}(\mathcal{E})$ equals $3/2(N+1)$, except for the state $j = (N+1)/2$, which gives $\mathcal{L}(\mathcal{E}) = 2/(N+1)$ (this band center state only occurs for N odd). To a good approximation, the latter values are also found in the numerical diagonalization of the homogeneous linear chain with *all* dipolar interactions included. Clearly, $\mathcal{L}(\mathcal{E})$ is not sensitive to small values of the site amplitude a_{jn} and therefore cannot prove the occurrence of true (Anderson) localization. $\mathcal{L}(\mathcal{E})$ should rather be regarded as a measure of the domain length over which the wave functions have a sizable amplitude.

III. DIAGONAL DISORDER

In this section we discuss our numerical results for diagonal disorder. We assume a Gaussian distribution with standard deviation D for the offset frequencies D_n ,

$$P(D_n) = (1/D\sqrt{2\pi}) \exp(-D_n^2/2D^2), \quad (3.1)$$

and regular molecule positions $r_n = na$. It is assumed that the offsets of different molecules are totally uncorrelated. Correlation effects will be discussed in the final part of this section.

As a typical example of the results of our simulations, we show in Fig. 1(a) the oscillator strengths of the states at the bottom of the band for a single inhomogeneous chain of 250 molecules at $D/J = 0.106$. Moreover, the site amplitudes of three of these states are plotted in Fig. 1(b). As one can see, only a few states possess a large oscillator strength, and the wave functions of these states are localized on segments of the chain. Clearly, describing these wave functions in terms of the totally delocalized wave functions of the homogeneous chain is inappropriate. The localized nature may further be demonstrated by the following example. The two wave functions in Fig. 1(b) which are roughly located on molecules 50 to 250, are hardly affected by choosing new

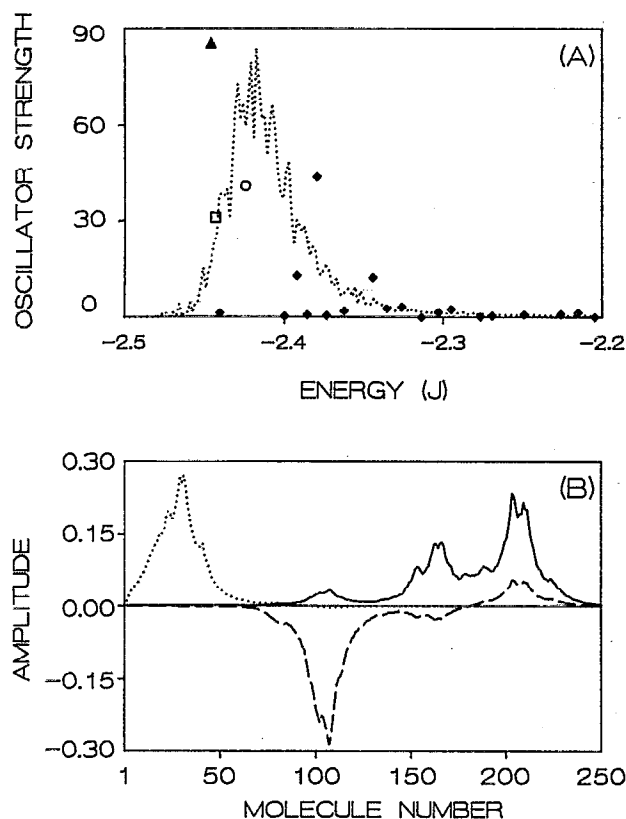


FIG. 1. (a) Oscillator strength (in units of μ_{mon}^2) against energy for the eigenstates at the bottom of the exciton band, found by diagonalizing one chain of 250 molecules with random site energies ($D/J = 0.106$). The dotted line is the absorption spectrum, at a resolution of $R = 1.7 \times 10^{-3}$ J, obtained by averaging over 500 chains. (b) Site amplitudes a_{jn} of the wave functions corresponding to three states selected from (a): (\blacktriangle , —); (\circ , ...), (\square , --).

random offsets for the first 50 molecules; in fact, the resulting changes in site amplitudes upon such a new choice turned out to be less than 0.5% for the molecules 70 to 250.

Also depicted in Fig. 1(a) (dotted line) is the total absorption line shape, calculated from Eq. (2.9) by averaging over 500 chains of 250 molecules, with a resolution $R = 1.7 \times 10^{-3}$ J. Comparing the single-chain results with the total absorption spectrum, nicely demonstrates that the total line shape is the statistical property of an ensemble of aggregates and cannot be thought of as a convolution of a "homogeneous" single aggregate absorption spectrum with an overall inhomogeneity function. Recent resonance light-scattering experiments on aggregates of PIC in an ethylene glycol/water glass showed that fluorescence, induced by exciting on the low-energy side of the absorption band, eventually extends over the full absorption line, which confirms these particular conclusions.^{6,14}

The same absorption spectrum is shown in Fig. 2(a), but now over a much larger part of the exciton band. In addition, an enlargement of the intraband tail is given in the inset of Fig. 2(a). For $J = 600 \text{ cm}^{-1}$ the main absorption band provides a good fit to the experimentally observed low-temperature absorption line shape for the aggregates of PIC in ethylene glycol/water glass.^{6,14} The main absorption band in Fig. 2(a) shows the typical asymmetry which has also been obtained in other theories.^{23,24,39} Its characteristics

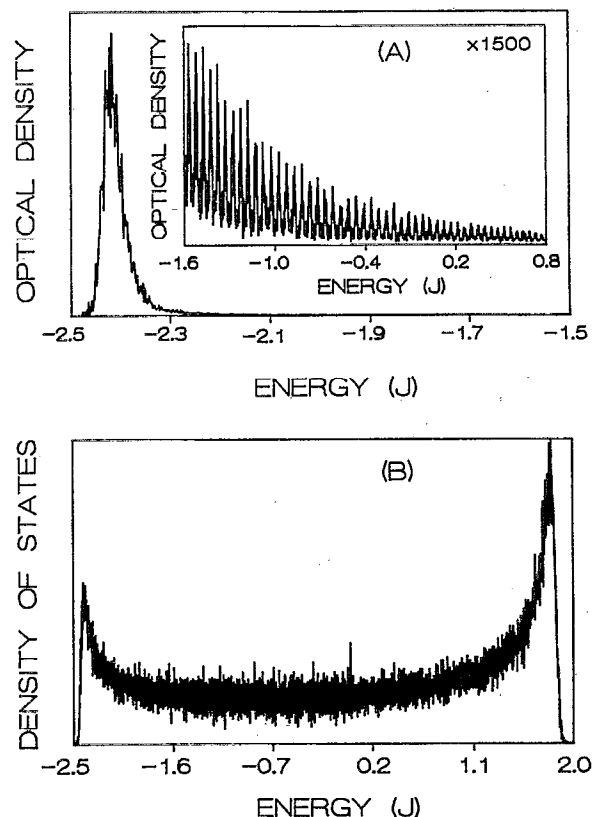


FIG. 2. (a) Absorption spectrum obtained by averaging over 500 chains of 250 molecules with diagonal disorder ($D/J = 0.106$). The inset shows the absorption spectrum at the central part of the exciton band at higher sensitivity. The energy resolution of both is $R = 1.7 \times 10^{-3}$ J. (b) Density of states for the same ensemble as in (a).

are a Gaussian line shape on the low-energy side and a Lorentzian line shape on the high-energy (intraband) side. The absorption maximum is red shifted by approximately 1.5×10^{-2} J relative to the lowest state of the homogeneous spectrum at -2.403 J. The enlargement of the intraband tail of the absorption spectrum shows regularly spaced Gaussian peaks, with the full width at half maximum (FWHM) given by $(1.8 \pm 0.3) \times 10^{-2}$ J. The continuously decreasing intensities of these peaks closely resembles the decreasing oscillator strength of the odd labeled j states of the homogeneous linear aggregate [Eq. (2.7)]. We also calculated the absorption spectrum for chains of 100 molecules (at the same value of D/J) and found that the main absorption peak was not strongly affected by this change of chain length. The spacing of the peaks in the tail, however, increased by a factor of 2.5. This suggests that, contrary to the states forming the main absorption band, the eigenstates at the central portion of the band can be viewed as perturbed homogeneous exciton states [for $D/J = 0.106$ and chain lengths of 100 and 250 molecules], which must have a fairly delocalized character. This idea is not only further demonstrated by calculating the degree of localization $\mathcal{L}(\mathcal{E})$ for these states (*vide infra*), but also by the fact that the widths of the intraband peaks approximately equal D/\sqrt{N} . This may be interpreted as exchange narrowing, resulting from averaging the Gaussian offset energies of the N molecules over which the excitation is delocalized.¹⁷ In practice it will

be difficult to observe the intraband absorption tail, because of overlap with vibrational transitions. Moreover, a distribution of chain lengths will wash out the spectral structure in the tail.

Figure 2(b) shows the density of states found from our simulations on aggregates of 250 molecules at $D/J = 0.106$ ($R = 1.7 \times 10^{-3}$ J). As discussed in Sec. II, the asymmetry around $\mathcal{E} = 0$ results from the inclusion of *all* dipolar interactions. The spiky nature of the density of states is not only caused by the limited statistics of the simulations, but also demonstrates again that the intraband eigenstates still bear a strong resemblance to the discrete eigenstates of the homogeneous system.

In Fig. 3 the degree of localization $\mathcal{L}(\mathcal{E})$ is plotted for ensembles of aggregates with $D/J = 0.106$ ($N = 100$ and $N = 250$) and $D/J = 0.425$ ($N = 250$). In the case $D/J = 0.106$, the $\mathcal{L}(\mathcal{E})$ values of states well inside the exciton band for both values of N are only 10%–20% higher than $3/2(N + 1)$. This indicates that the typical intraband eigenstates are almost completely delocalized over the chain at this inhomogeneous width. Near the band edges, the states are much more localized.^{24,25} This is also nicely demonstrated by the following observation: inside the band, $\mathcal{L}(\mathcal{E})$ is almost 2.5 times higher for the 100 molecule chains than for the 250 molecule chains, whereas at the band edges the difference vanishes. For $D/J = 0.425$, on the other hand, the

intraband wave functions are not delocalized over the entire chain, as is clear from the overall increase of $\mathcal{L}(\mathcal{E})$ in Fig. 3(b) compared to Fig. 3(a). Thus, in general, the delocalization length can be limited by either the chain length (N) or by the inhomogeneity (D/J). If D/J grows, the number of states inside the band for which the chain length still limits the delocalization length gets smaller. Of course, this physically very intuitive result plays no role in the theory of Anderson localization on infinite chains, but it *is* important for real aggregates with finite lengths. It follows that also aggregate properties, such as the absorption line shape and the enhancement of the radiative decay rate, can be determined by D/J alone, or by N as well. For example, we already mentioned that the main absorption band is the same for $N = 100$ and $N = 250$ at $D/J = 0.106$. The reason is that this absorption peak is located at the lower band edge, where the states are (on the average) localized on less than 100 molecules.

We have investigated the D/J dependence of the absorption band width (FWHM), the shift of the absorption maximum relative to the homogeneous case, and the two measures for the radiative enhancement introduced in Sec. II. Within the studied inhomogeneity interval ($D/J = 0.053$ to 0.425), these quantities are not determined by the chain

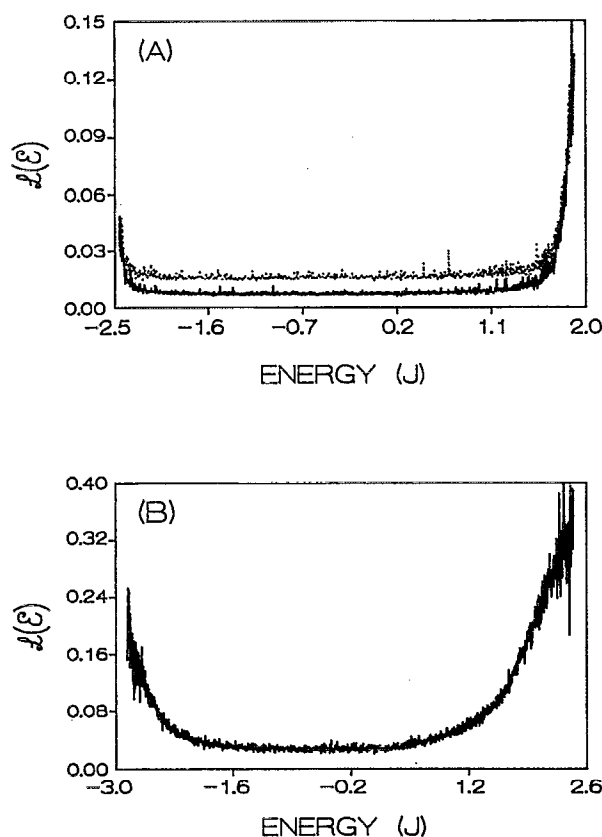


FIG. 3. (a) Degree of localization $\mathcal{L}(\mathcal{E})$ for diagonal disorder with $D/J = 0.106$ for chains of 100 molecules (\cdots) and 250 molecules ($—$), both with a resolution $R = 1.7 \times 10^{-3}$ J. (b) As (a), with $D/J = 0.425$ and chains of 250 molecules.

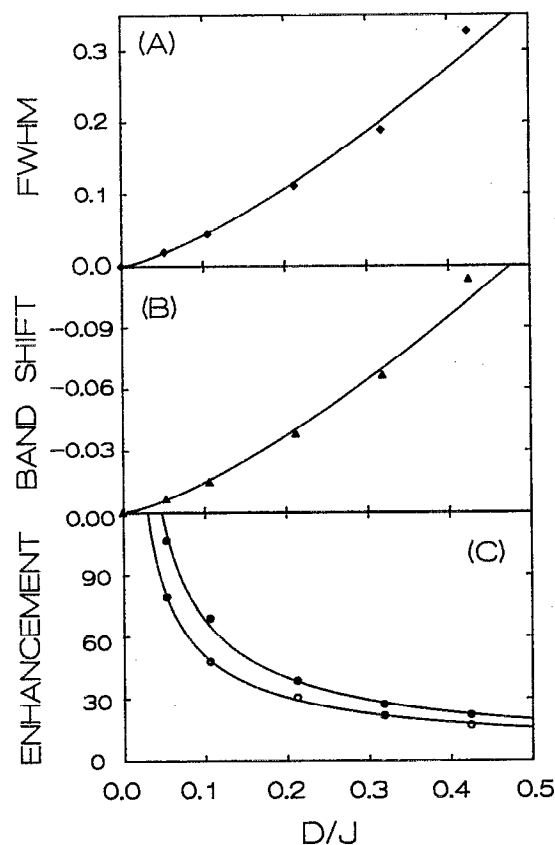


FIG. 4. (a) D/J dependence of the FWHM of the absorption band (in units of J). (b) D/J dependence of the shift of the absorption band (in units of J). (c) D/J dependencies of the radiative enhancements $\max(\mu_{av}^2)$ (O) and μ_{echo}^2 (●) (both in units of μ_{mon}^2). Parameters corresponding to the fits are listed in Table I. (All calculations were performed on chains of 250 molecules.)

TABLE I. Diagonal disorder: D/J dependence of the various quantities discussed in the text when fitted to the expression $c(D/J)^\alpha$.

	c	α
Absorption band		
FWHM	$0.94J$	1.34
Shift	$-0.33J$	1.35
Radiative enhancement		
$\max(\mu_{av}^2)$	$9.3\mu_{mon}^2$	-0.74
μ_{echo}^2	$11.5\mu_{mon}^2$	-0.77

length of 250 molecules anymore. At every value of D/J at least 150 aggregates were diagonalized. The results are summarized in Fig. 4. The curves in these figures represent fits of the form $c(D/J)^\alpha$, where c is expressed in units of J for the width and the shift, and in units of μ_{mon}^2 for the radiative enhancement. The values found for c and α are given in Table I; all values for α can be varied by 10%, while still maintaining good fits. In all cases the echo decay was considered at the energy where μ_{av}^2 is maximum. It is to be noted from Table I that the enhancement of the radiative rate as determined from fluorescence experiments [$\max(\mu_{av}^2)$] and by photon-echo experiments (μ_{echo}^2) have about the same D/J dependence. Fitting the data with the same power α shows that the echo always decays roughly 30% faster than the fluorescence. For $D/J = 0.106$, the calculated enhancement is in good agreement with the earlier mentioned experiments on PIC aggregates.¹⁴ Note that the obtained power laws for the enhancement measures do not recover the rate $0.83N\mu_{mon}^2$ for $D/J = 0$, because they have been derived for D/J large enough so that the chain length N does not limit the delocalization. Padé-like expressions that also cover the limit $D/J = 0$, are easily constructed and lead to enhancements of the form

$$0.83N\mu_{mon}^2 / \{1 + 0.83N\mu_{mon}^2 [c(D/J)^\alpha]^{-1}\},$$

with c and α taken from Table I.

Using perturbation theory and numerical simulations for chains of 10 and 40 molecules, Spano and Mukamel¹⁸ concluded that the radiative decay rate *per molecule* for the lowest state in the exciton band ($\Gamma_1/N \propto \mu_1^2/N$) depends on the chain length and the inhomogeneity only through a single parameter,

$$\hat{\Gamma}_1/N = f(N^{3/2}D/J). \quad (3.2)$$

We found above, however, that for N large and (or) D/J large, all N dependence vanishes for properties of states near the band edges. The scaling equation (3.2) can still be reconciled with this conclusion if the function $f(x)$ for $x \gg 1$ drops off as $x^{-2/3}$. This would lead to a power $\alpha = -\frac{2}{3}$ for the radiative enhancement, which is indeed in fair agreement with our numerically obtained values in Table I. Only if the delocalization length of the states near the band edges is smaller than the number of molecules, will the enhancement also be a determined N .

The values of α for the FWHM and the radiative enhancement in Table I can be related in a simple way using the concept of exchange narrowing.¹⁷ According to this concept, the FWHM of the main absorption band is given by

$(8 \ln 2)^{1/2} D / \sqrt{N_{del}}$, with N_{del} , the delocalization length of the exciton states. It is reasonable to assume that near the absorption peak, N_{del} is roughly given by (or at least proportional to) the radiative enhancement factor, which scales as $(D/J)^{-0.74}$. Thus, the FWHM is expected to be proportional to $J(D/J)^{1.37}$, which agrees surprisingly well with the independently obtained fit parameter $\alpha_{FWHM} = 1.34$. This value also agrees very well with previous results derived by Schreiber and Toyozawa²⁴ (using renormalized first-order perturbation theory), by Boukahl and Huber²⁶ (using the coherent potential approximation), and by Köhler *et al.*²⁷ (using numerical simulations) that $\alpha_{FWHM} = \frac{4}{3}$. The proportionality constants obtained by these authors are $c_{FWHM} = 1.09J$ (Ref. 26) and $c_{FWHM} = 1.26J$ (Refs. 24 and 27). On the other hand, our D/J dependence of the band shift does *not* agree with the (initial) linear dependence predicted by Schreiber and Toyozawa,²⁴ but it almost perfectly coincides with Boukahl and Huber's²⁶ result: Shift = $-0.315J(D/J)^{4/3}$. It should be noted that all these theories only include nearest-neighbor interactions $-J$. Apparently, inclusion of all dipolar couplings (instead of only the nearest-neighbor ones) does not at all affect the power of the D/J dependencies of the absorption width and shift; even the proportionality constants c are changed by at most about 30% by this.

The effect of longer-range interactions, however, seems much more important for the radiative enhancement. For these quantities, no comparison to previous results can be made, except that, as explained earlier, the powers α are in reasonable agreement with the scaling hypothesis (3.2). However, a proportionality constant cannot be deduced from this. Therefore, we made a direct comparison by performing, for the particular case of $D/J = 0.106$, new simulations with only nearest-neighbor interactions. We found that $\max(\mu_{av}^2)$ then decreases from $49\mu_{mon}^2$ to $22\mu_{mon}^2$ and μ_{echo}^2 decreases from $69\mu_{mon}^2$ to $24\mu_{mon}^2$. Thus, neglecting the long-range nature of the dipolar interactions results in predictions of the radiative enhancement that are low by more than a factor 2.

So far, we have assumed that the Gaussian disorder is totally uncorrelated for different molecules within an aggregate. Knapp¹⁷ performed a theoretical study of the influence of correlated diagonal disorder on the absorption linewidth. It is evident that an ensemble of aggregates with perfectly correlated offsets D_n within each individual aggregate (i.e., all molecules within a given aggregate have the same offset randomly chosen for that aggregate), results in an absorption spectrum that is the convolution of the homogeneous aggregate spectrum and the (Gaussian) inhomogeneous distribution of offsets. Consequently, the FWHM of the main absorption band is then no longer given by the exchange narrowing value $[(8 \ln 2)^{1/2} D / N^{1/2}]$, but rather by the FWHM of the Gaussian distribution, $(8 \ln 2)^{1/2} D \approx 2.35D$. Moreover, in the case of perfect correlation, the lowest state of each aggregate will be superradiant with a radiative decay rate given by $0.83N$ times the monomer rate.

We have investigated the effects of correlations in the diagonal disorder on the various optical properties. To this end, we performed simulations for $D/J = 0.106$ ($N = 250$),

TABLE II. Correlation effects in the FWHM of the absorption band and the two radiative enhancement measures at $D/J = 0.106$ for chains of 250 molecules. "Average step" is the average offset difference of neighboring molecules and $\delta D_{\max} = \infty$ indicates the completely uncorrelated case.

δD_{\max}	Average step (D)	FWHM (10^{-2} J)	$\max(\mu_{\text{av}}^2)$ (μ_{mon}^2)	μ_{echo}^2 (μ_{mon}^2)
∞	$(4/\pi)^{1/2} = 1.13$	4.5	49	69
$D/2$	0.24	15.8	30	38
$D/4$	0.13	19.2	27	47
$D/8$	0.06	16.7	29	60

in which we introduced correlations by imposing an upper limit δD_{\max} on the offset differences $|D_n - D_{n+1}|$ for adjacent molecules. From the results, given in Table II, it is seen that with growing correlation the absorption linewidth rapidly increases, confirming the expected vanishing of exchange narrowing. (The decrease of the linewidth from $\delta D_{\max} = D/4$ to $\delta D_{\max} = D/8$ is due to particularly poor statistics for the latter case.)

The results for μ_{echo}^2 show a less intuitive behavior. In the presence of correlations, the chain will contain a sequence of more or less ordered intervals (fragments), within each of which the molecules have similar offsets, so that the excitation easily delocalizes over it. With growing correlations, the typical size of these intervals increases and we expect a monotonous increase of μ_{echo}^2 . In contrast to this, we see a sharp initial drop in μ_{echo}^2 between $\delta D_{\max} = \infty$ and $\delta D_{\max} = D/2$. This may be understood from the fact that the differences in the average offset between two chain fragments grows when going from a situation without correlations to one with correlations. Thus, it gets more difficult for the excitation to be delocalized over several fragments, which at small fragment sizes (δD_{\max} large) limits μ_{echo}^2 . At smaller values of δD_{\max} , the expected monotonous increase is indeed observed. The limiting value for perfect correlation is $\mu_{\text{echo}}^2 = 0.83N\mu_{\text{mon}}^2$.

In contrast to μ_{echo}^2 , $\max(\mu_{\text{av}}^2)$ does not reflect the length over which offsets are correlated. Instead, $\max(\mu_{\text{av}}^2)$ becomes independent of δD_{\max} as soon as the correlation length gets large enough to prevent noticeable narrowing of the Gaussian distribution of offsets (absorption linewidth $\approx (8 \ln 2)^{1/2}D$). This is clearly demonstrated by ensembles of perfectly correlated aggregates, for which the normalized density of states and absorption spectrum [based on Eqs. (2.6b) and (2.7), together with the distribution function (3.1)] are nearly independent of chain length N and therefore also $\max(\mu_{\text{av}}^2)$, which is obtained by dividing these, does not depend on N .

IV. OFF-DIAGONAL DISORDER

The preceding section dealt exclusively with disorder in the transition energies of the individual molecules within the chain. A different source for disorder lies in the interaction terms J_{nm} . Interaction or off-diagonal disorder can be caused by randomness in either the molecular orientation or the molecular positions. In this section we investigate off-

diagonal disorder originating from a Gaussian distribution of the positions around regular lattice points,

$$P(r_n) = (1/\sigma a \sqrt{2\pi}) \exp[-(r_n - na)^2/2(\sigma a)^2]. \quad (4.1)$$

As before, a is the average nearest-neighbor distance; σa is the standard deviation of the distribution, so that σ is the dimensionless measure for the magnitude of the disorder (cf. D/J in Sec. III). The nearest-neighbor distance $r_{n+1} - r_n$ obeys a Gaussian distribution with average a and standard deviation $\sigma a \sqrt{2}$. Although positional disorder is most likely accompanied by some amount of diagonal disorder, we take $D_n = 0$ for all molecules in this section, in order to isolate the effects of off-diagonal disorder only. Some results on systems with diagonal and off-diagonal disorder will be given in the last part of this section.

Of course, the randomness in the intermolecular distances induced by the distribution Eq. (4.1), mainly affects the interactions $J_{n,n+1}$ between neighboring molecules. Using Eq. (2.3), we obtain, for the probability distribution function of these interactions,

$$P(J_{n,n+1}) = (1/3\sigma J \sqrt{4\pi}) (-J/J_{n,n+1})^{4/3} \times \exp\left(-\frac{[(-J/J_{n,n+1})^{1/3} - 1]^2}{4\sigma^2}\right). \quad (4.2)$$

As a result of the $1/r^3$ dependence of the dipolar interaction, this distribution is not symmetrical, but has a long tail towards large nearest-neighbor interactions (Fig. 5). Further analysis shows that for $\sigma \ll 1$ the peak of the distribution Eq. (4.2) is found at $J_{n,n+1} = -J(1 - 24\sigma^2)$, the average value is given by $\langle J_{n,n+1} \rangle = -J(1 + 12\sigma^2)$, and the standard deviation is given by $\sigma_J = 3\sqrt{2}\sigma J$. The latter equality means that also in terms of energy, the disorder is linear in σ .

We have performed simulations on ensembles of linear chains of 250 molecules. Figure 6(a) shows the absorption spectrum for $\sigma = 0.08$, at a resolution $R = 5 \times 10^{-3}$ J. In contrast to Sec. III, this spectrum shows a Lorentzian-like line shape on the low-energy side, which reflects the tail of

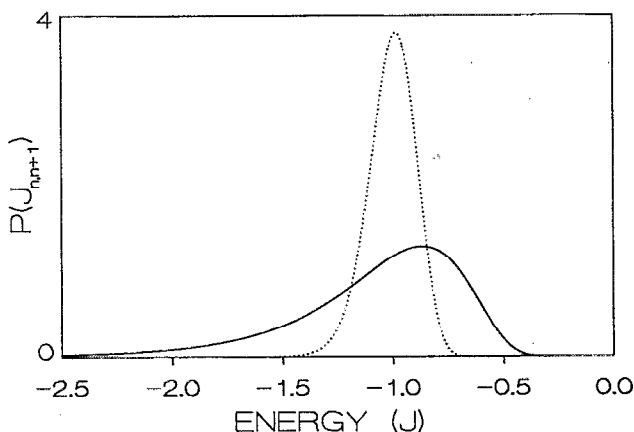


FIG. 5. Normalized distribution function for the nearest-neighbor interaction [Eq. (4.2)] for $\sigma = 0.025$ (···) and $\sigma = 0.08$ (—).

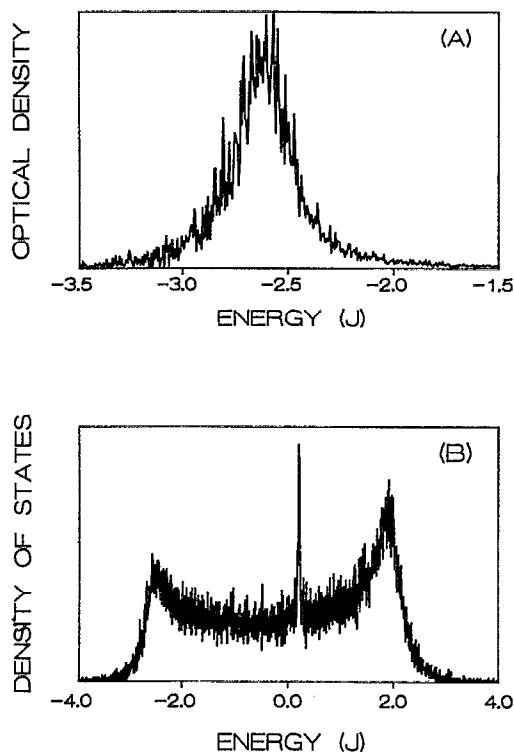


FIG. 6. (a) Absorption spectrum, obtained by averaging over 160 chains of 250 molecules with off-diagonal disorder ($\sigma = 0.08$). The resolution is $R = 5 \times 10^{-3}$ J. (b) Density of states corresponding to the situation of Fig. 6(a).

the distribution function, Eq. (4.2). It is interesting to note that absorption spectra of PIC in Langmuir–Blodgett films indeed show such a tail.⁴⁰ In Fig. 6(b) we give the density of states (DOS) found from the same simulations. As before, this quantity exhibits an asymmetry mainly caused by the long range of the dipolar interactions. For aggregates with only random nearest-neighbor interactions (distributed according to a step function²⁸ or a generalized Poisson distribution²⁹), it has been proved that a singularity occurs in the DOS at $\mathcal{E} = 0$. Figure 6(b) clearly shows that this feature also exists for the asymmetrical distribution (4.2) and with inclusion of all dipolar couplings, but that it is shifted to a somewhat higher energy, $\mathcal{E} = 0.21$ J. This shift agrees very well with the energy of the central band states for circular aggregates ($j = N/4$ or $j = 3N/4$), which for dipolar interactions equals $\mathcal{E}_j^C = 0.225J$ [Eq. (2.8b)] and vanishes if only nearest-neighbor interactions are included. This strongly suggests that the shift is caused by the inclusion of *all* dipolar interactions on the chain and that in general the singularity in the DOS is not specifically related to $\mathcal{E} = 0$, but rather to a specific form of the (unperturbed) wave function.

Figure 7 shows the degree of localization for $\sigma = 0.08$. As in the case of diagonal disorder, we see that the intraband states are more delocalized than the states at the band edges. At the band edges, $\mathcal{L}(\mathcal{E})$ approaches 0.5, in contrast to diagonal disorder, where the limiting value of $\mathcal{L}(\mathcal{E})$ equals unity (not shown in Fig. 3). This may easily be understood. In the case of diagonal disorder, the states far outside the

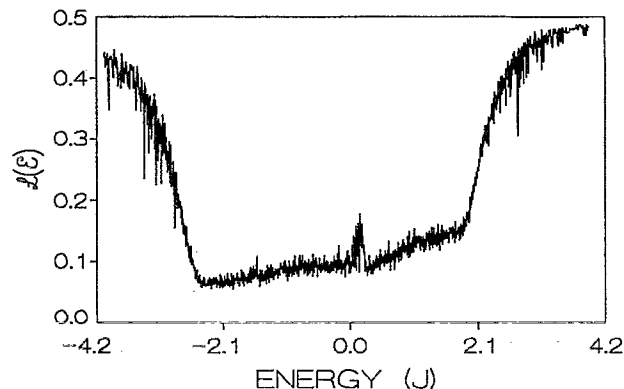


FIG. 7. Degree of localization $\mathcal{L}(\mathcal{E})$ as a function of energy in the case of off-diagonal disorder with $\sigma = 0.08$, resulting from averaging over 160 chains of 250 molecules (same ensemble as Fig. 6). The resolution is $R = 5 \times 10^{-3}$ J.

band are localized on a single molecule that happens to have a large energy offset. In the case of off-diagonal disorder, on the other hand, the strong interaction tail of Eq. (4.2) corresponds to a large reduction of the distance between two adjacent molecules. For $\sigma = 0.08$, it is unlikely that simultaneously the distance with the other neighbors is strongly reduced. Therefore, strongly interacting “dimers” are created on the chain, in agreement with $\mathcal{L}(\mathcal{E}) = 0.5$. This formation of coupled pairs resembles the concept of excimers.⁴¹ Another new feature, is the gradual increase of $\mathcal{L}(\mathcal{E})$ with growing energy in the intraband part of Fig. 7. We have no explanation for this.

More interesting seems to be the peak near the energy where also the DOS peaks. At first glance, this contradicts the result^{29,30} that the states near the singularity in the DOS (in the case of random nearest-neighbor interactions) are completely delocalized. It should be pointed out, however, that also for homogeneous aggregates the localization measure $\mathcal{L}(\mathcal{E})$ has a higher value at the center of the band than at all other states [see the discussion following Eq. (2.14)]. This state is, however, no more localized than other states of the homogeneous chain; it is well characterized by the wave function $[2/(N+1)]^{1/2} \sin(n\pi/2)$, which explains an effective dilution of the linear chain, as half the molecules have no amplitude at all. We are convinced that the peak in Fig. 7 is a remnant of this special state.

In analogy to Sec. III, we have studied the disorder (σ) dependencies of the absorption band width (FWHM), the shift of the absorption maximum relative to the homogeneous case, and the two measures for the radiative enhancement. Again the echo decay was considered at the energy where μ_{av}^2 is maximum. The chain length of 250 molecules is large enough, so that it does not determine the values of the observables in the studied inhomogeneity interval ($\sigma = 0.025$ to 0.08) anymore. At least 100 aggregate configurations were diagonalized for each value of σ . The results are given in Fig. 8, together with fits of the form $c\sigma^\alpha$. As in Sec. III, the values of α can be varied by 10%, without severely affecting the quality of the fits.

As for the case of diagonal disorder, $\max(\mu_{av}^2)$ and μ_{echo}^2

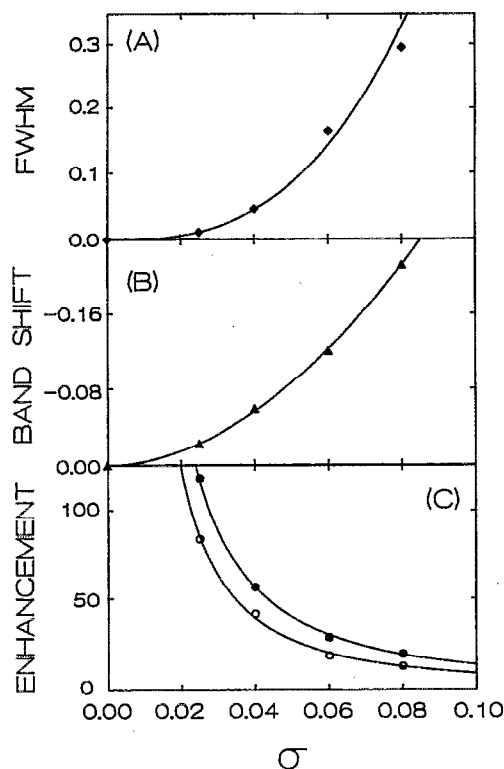


FIG. 8. (a) σ dependence of the FWHM of the exciton absorption band (in units of J). (b) σ dependence of the shift of the absorption band (in units of J). (c) σ dependencies of the radiative enhancements $\max(\mu_{av}^2)$ (\circ) and μ_{echo}^2 (\bullet) (both in units of μ_{mon}^2). Parameters corresponding to the fits are listed in Table III. (All calculations were performed on chains of 250 molecules.)

show approximately the same σ dependence; fitting the data of both enhancement measures with the same value of α , we now find that μ_{echo}^2 is about 45% larger than $\max(\mu_{av}^2)$. Moreover, the decrease of the radiative enhancement with increasing σ is much steeper than with increasing D/J (the power α is about two times higher than in the case of diagonal disorder).

It is noteworthy that the absorption band shift caused by the configurational disorder can almost completely be explained by the shift in the average nearest-neighbor interaction, which equals $\langle J_{n,n+1} \rangle + J = -12J\sigma^2$. These extra nearest-neighbor interactions would shift the band edge over $-24J\sigma^2$, which is in very good agreement with the σ dependence given in Table III. Striking is the strong σ dependence of the FWHM of the absorption band, expressed by the power $\alpha_{FWHM} = 2.84$. We furthermore note that, unlike the

TABLE III. Off-diagonal disorder: σ dependence of the various quantities discussed in the text when fitted to the form $c\sigma^\alpha$.

	c	α
Absorption band		
FWHM	$425J$	2.84
Shift	$-25J$	1.89
Radiative enhancement		
$\max(\mu_{av}^2)$	$0.20\mu_{mon}^2$	-1.64
μ_{echo}^2	$0.39\mu_{mon}^2$	-1.55

case of diagonal disorder, for the present case of off-diagonal disorder the exchange narrowing argument in combination with the disorder (σ) dependence of $\max(\mu_{av}^2)$ does not give good agreement with the observed σ dependence of the FWHM. This is not surprising, because the \sqrt{N} exchange narrowing factor is specific for a Gaussian distribution function. Tilgner *et al.*⁹ numerically simulated the absorption spectrum of polysilane, with a Gaussian distribution for D_n and with a Gaussian distribution for $J_{n,n+1}$ (both with only nearest-neighbor interactions). They claim to find similar results for both types of disorder. In contrast, our results for diagonal and off-diagonal disorder are very different. Of course, part of this discrepancy lies in the fact that we do not assume a Gaussian distribution for the interactions, but instead introduce the off-diagonal disorder through a distribution of the molecular positions. In our opinion, this is a more physical way to incorporate interaction disorder.

In practice, off-diagonal disorder will be accompanied by diagonal disorder. It is therefore interesting to know if (and how) the optical properties in the presence of both types of disorder, can be related to the cases with only one type of disorder. Therefore, we have performed preliminary calculations on combined diagonal and off-diagonal disorder. From these, we find that the total band shift is the sum of the shifts caused by the diagonal and off-diagonal disorder separately, whereas the absorption bandwidth turns out to be the geometric mean of the separate bandwidths. (This prescription corresponds to an addition of independent Gaussian broadening mechanisms.) For the radiative enhancement a less clear cut recipe is found. To a good approximation, the smallest of the two enhancements obtained for either diagonal or off-diagonal disorder separately can be taken; the maximum decrease compared to this value is approximately 25%. Generally, we find that in case of a large difference in quantitative effect of diagonal and off-diagonal disorder on the optical property of interest, it is determined by only one. It should further be noted that no peak in the density of states is observed at $\mathcal{E} = 0.21J$ with both types of disorder present.

V. SUMMARY

Using straightforward numerical simulations, we have studied the effect of diagonal and off-diagonal disorder on optical properties of linear molecular aggregates. The two independent parameters in our theory are the chain length (N) and the magnitude of the disorder relative to the intermolecular interactions (D/J for diagonal disorder and σ for off-diagonal disorder). In contrast to previous studies, off-diagonal disorder is introduced through randomness in the molecular positions, as in our opinion this is an important physical origin of disordered interactions. Disorder tends to localize the eigenstates (Frenkel excitons) on segments of the chain. From the degree of localization (inverse participation ratio), it is seen that the states at the band edges are relatively strongly localized, whereas the intraband states are much more delocalized (quasiextended).²⁵ The extension of the intraband states is also nicely demonstrated by their exchange narrowing. The optical properties of aggregates are predominantly determined by the states at the band

edges, because the oscillator strength is concentrated there. Thus, if the delocalization length at the band edges is smaller than the aggregate length, the optical properties do not depend on N . This explains why experimental fluorescence decays are often monoexponential, despite the fact that, in practice, we deal with a distribution of chain lengths. Conversely, this implies that N can only be assessed from optical experiments if the chain length is shorter than the delocalization length.

In order not to convolute their effects, we have separately studied diagonal and off-diagonal disorder; only preliminary calculations on combined disorder were presented. In general, it appears that off-diagonal disorder has a stronger effect on the optical observables than diagonal disorder [the powers α expressing the disorder dependence through $(D/J)^\alpha$ and σ^α are higher in the latter case]. This most likely results from the strong-interaction tail in the asymmetric distribution (4.2) for the nearest-neighbor interactions. It seems that diagonal disorder plays a dominant role for linear polymers,⁹ self-organized aggregates in glasses^{6,14} and triplet excitons in molecular solids,⁴² whereas off-diagonal disorder is more important in Langmuir–Blodgett films,⁴⁰ which are forced into a configuration by applying an external force on a monolayer of molecules. These ideas are confirmed by the fact that a Lorentzian low-energy tail, as in Fig. 6(a), has indeed been observed in the absorption spectrum of Langmuir–Blodgett films of PIC.⁴⁰ Furthermore, the low-temperature absorption line shape, superradiant emission, and resonance light scattering on self-formed aggregates of PIC in a glassy environment,^{6,12,14} can be understood from our calculations on diagonal disorder only.

Contrary to all previous studies, we did not restrict to nearest-neighbor interactions, but considered *all* dipolar interactions between the molecules on the chain. We have shown that this causes an asymmetry in the DOS (even for homogeneous systems). In the case of diagonal disorder, comparison to previous work on the absorption line shows that the dependence of the absorption linewidth and line shift on the disorder D/J are hardly affected by this inclusion of longer range interactions. The superradiant behavior of the aggregates, on the other hand, shows a very strong effect. In the case of off-diagonal disorder, we could not assess the effect of the longer-range interactions, as, to our knowledge, no systematic study of the optical properties of such a system has been performed before. One very interesting, and as yet not understood effect of these extra interactions in the case of off-diagonal disorder, is that the singularity found in the DOS for such systems shifts away from $\mathcal{E} = 0$. Finally, we note that we neglected the role of phonons in this paper. In order to explain any temperature dependence of the observables, the inclusion of phonons is of course essential.

ACKNOWLEDGMENTS

We gratefully acknowledge Foppe de Haan for providing us with useful data processing software. This research

was supported by the Netherlands Foundations for Chemical Research (SON) and Physical Research (FOM) with financial aid from the Netherlands Organization for Scientific Research (NWO). One of the authors (J.K.) gratefully acknowledges support by the NWO through the award of a Huygens fellowship.

- ¹ E. Hanamura, *Phys. Rev. B* **37**, 1273 (1988).
- ² F. C. Spano and S. Mukamel, *Phys. Rev. Lett.* **66**, 1197 (1991).
- ³ J. Feldmann, G. Peter, E. O. Göbel, P. Dawson, K. Moore, C. Foxon, and R. J. Elliott, *Phys. Rev. Lett.* **59**, 2337 (1987).
- ⁴ D. Möbius and H. Kuhn, *Isr. J. Chem.* **18**, 375 (1979).
- ⁵ J. Terpstra, H. Fidder, and D. A. Wiersma, *Chem. Phys. Lett.* **179**, 349 (1991).
- ⁶ H. Fidder, J. Terpstra, and D. A. Wiersma, *J. Chem. Phys.* **94**, 6895 (1991).
- ⁷ R. D. Miller and J. Michl, *Chem. Rev.* **89**, 1359 (1989).
- ⁸ J. R. G. Thorne, Y. Osaka, J. M. Zeigler, and R. M. Hochstrasser, *Chem. Phys. Lett.* **162**, 455 (1989).
- ⁹ A. Tilgner, H. P. Trommsdorff, J. M. Zeigler, and R. M. Hochstrasser, *J. Lumin.* **45**, 373 (1990).
- ¹⁰ S. de Boer, K. J. Vink, and D. A. Wiersma, *Chem. Phys. Lett.* **137**, 99 (1987).
- ¹¹ S. de Boer and D. A. Wiersma, *Chem. Phys.* **131**, 135 (1989).
- ¹² S. de Boer and D. A. Wiersma, *Chem. Phys. Lett.* **165**, 45 (1990).
- ¹³ H. Fidder, J. Knoester, and D. A. Wiersma, *Chem. Phys. Lett.* **171**, 529 (1990).
- ¹⁴ H. Fidder and D. A. Wiersma, *Phys. Rev. Lett.* **66**, 1501 (1991).
- ¹⁵ R. Hirschmann, J. Friedrich, and E. Daltrozzo, *J. Chem. Phys.* **91**, 7296 (1989).
- ¹⁶ V. Sundström, T. Gillbro, R. A. Gadonas, and A. Piskarskas, *J. Chem. Phys.* **89**, 2754 (1988).
- ¹⁷ E. W. Knapp, *Chem. Phys.* **85**, 73 (1984).
- ¹⁸ F. C. Spano and S. Mukamel, *J. Chem. Phys.* **91**, 683 (1989).
- ¹⁹ G. I. Stegeman, C. T. Seaton, and R. Zanon, *Thin Solid Films* **152**, 231 (1987).
- ²⁰ M. Thakur and D. M. Krol, *Appl. Phys. Lett.* **56**, 1213 (1990).
- ²¹ N. F. Mott and W. D. Twose, *Adv. Phys.* **10**, 107 (1961).
- ²² R. Landauer, *Philos. Mag.* **21**, 863 (1970).
- ²³ J. Klafter and J. Jortner, *J. Chem. Phys.* **68**, 1513 (1978).
- ²⁴ M. Schreiber and Y. Toyozawa, *J. Phys. Soc. Jpn.* **51**, 1528 (1981); **51**, 1537 (1981).
- ²⁵ M. Schreiber, in *Proceedings of the Localization 1990 Conference*, (London, 1990), *Inst. Phys. Conf. Ser. No. 108*, p. 65.
- ²⁶ A. Boukahil and D. L. Huber, *J. Lumin.* **45**, 13 (1990).
- ²⁷ J. Köhler, A. M. Jayannavar, and P. Reineker, *Z. Phys. B* **75**, 451 (1989).
- ²⁸ M. Weissmann and N. V. Cohan, *J. Phys. C* **8**, L145 (1975).
- ²⁹ G. Theodorou and M. H. Cohen, *Phys. Rev. B* **13**, 4597 (1976).
- ³⁰ P. D. Antoniou and E. N. Economou, *Phys. Rev. B* **16**, 3768 (1977).
- ³¹ J. D. Bauer, V. Logovinsky, and J. L. Skinner, *J. Phys. C* **21**, L993 (1988).
- ³² E. N. Economou and M. H. Cohen, *Phys. Rev. B* **4**, 396 (1971).
- ³³ D. H. Dunlap, K. Kundu, and P. Phillips, *Phys. Rev. B* **40**, 10999 (1989).
- ³⁴ P. W. Anderson, *Phys. Rev.* **109**, 1492 (1958).
- ³⁵ See, for instance, R. H. Lehmberg, *Phys. Rev. A* **2**, 883 (1970); J. Knoester and S. Mukamel, *ibid.* **40**, 7065 (1989).
- ³⁶ R. M. Hochstrasser and J. D. Whiteman, *J. Chem. Phys.* **56**, 5945 (1972).
- ³⁷ W. H. Press, B. P. Flannery, S. A. Teukolsky, and W. T. Vetterling, *Numerical Recipes* (Cambridge University, London, 1987), Chaps. 7 and 11.
- ³⁸ D. J. Thouless, *Phys. Rep.* **13**, 93 (1974).
- ³⁹ D. L. Huber, *Chem. Phys.* **128**, 1 (1988).
- ⁴⁰ J. Terpstra (private communication).
- ⁴¹ H. Port, R. Seyfang, and H. C. Wolf, *J. Phys. (Paris) Colloq.* **46**, C7-391 (1985).
- ⁴² D. M. Burland, U. Konzelmann, and R. M. Macfarlane, *J. Chem. Phys.* **67**, 1926 (1978).